

SUN Quan, JIANG Hong-bing, LIU Yi,
WU Zhao-xin, YANG Hong, GONG Qi-huang

Diagnose Parameters of Plasma Induced by Femtosecond Laser Pulse in Quartz and Glasses

© Higher Education Press and Springer-Verlag 2006

Abstract Electron plasma induced by a focused femtosecond pulse (130 fs, 800 nm) in quartz, fused silica, K9 glass, and Soda Lime glass was investigated by pump-probe technology. Pump and probe shadow imaging and interferometric fringe imaging have been used to determine plasma density, relaxation time, and electron collision time in the conduction band. In these materials, the electron collision time is about several femtoseconds when the electron density is in the 10^{19}cm^{-3} range. The electron relaxation processes are different: lifetime is about 170 fs in pure quartz and fused silica, and about 100 ps in K9 and Soda Lime glass. The modified electron band by doped ions is regarded to be responsible for the difference of decay time in these materials.

Keywords femtosecond laser pulse, plasma, electron collision time, electron density, electron relaxation process

PACS numbers 52.20.Fs, 52.38.Dx, 78.47.+p, 72.20.Jv

With the development of ultrafast laser technology, the interaction of focused femtosecond laser pulses with dielectric materials has attracted great attention recently. There are many new phenomena in this area, such as microexplosion [1], filamentation [2], and dielectric index modulation [3]. These phenomena have been widely studied because of their potential application in the fabrication of microstructures and integrated microoptics. Many microoptics have been fabricated, such as waveguide [3–6],

coupler [7,8], diffractive component [9,10], data storage [1,11], microfluid instrument [12], and microlaser [13]. In these applications, electron plasma is always induced and plays important roles. There are many studies on plasma. Ionization dynamics has been calculated [14], and the relation between the energy threshold to generate plasma and pulse duration has been measured and simulated [15]. However, there are seldom experimental measuring on electron parameters, such as electron collision time, electron density [16], and electron relaxation lifetime [17–19].

The electron collision time is important in the interaction. It dominates electron absorption and avalanche ionization rate. In fused silica, various magnitudes of τ were employed in different reports and calculations; for example, 23.3 fs was used by Sudrie et al. [20], 10 fs (obtained from the inverse Bremsstrahlung cross section $\sigma = 2.78 \times 10^{-18} \text{ cm}^2$) was used by Tzortzakis et al. [21], and 0.2 fs was used by Mao et al. [16].

The electron density in glasses is 10^{21} cm^{-3} during breakdown induced by nanosecond pulse [22] and is regarded as in the 10^{19} cm^{-3} [15] induced by femtosecond pulse. These data are important for understanding ionization mechanism and laser-induced structure change inside the transparent materials. This was measured to be $5 \times 10^{19} \text{ cm}^{-3}$ by Mao et al. [16] using shadow imaging. However, the formula used to determine the electron density from the shadowgraph is also related to the electron collision time τ , which was chosen as 0.2 fs by Mao et al. [16].

The electron relaxation process is crucial for energy transfer. It was measured in fused silica [17–19], and its lifetime is about 150 fs. Plasma-induced deep trap state is regarded to be responsible for this short lifetime [17,23,24]. Regarding other glasses, we have not found any experimental data.

In this paper, we review our work on measuring different plasma parameters, electron density, electron collision time, and electron relaxation time, in quartz and different glasses [19,25]. The time-resolved shadowgraph and interferometric fringe measurement were used.

SUN Quan, JIANG Hong-bing (✉), LIU Yi, WU Zhao-xin, YANG Hong, GONG Qi-huang (✉)
State Key Laboratory for Mesoscopic Physics,
Department of Physics, Peking University,
Beijing 100871, China
E-mail: hbjiang@pku.edu.cn, ghgong@pku.edu.cn

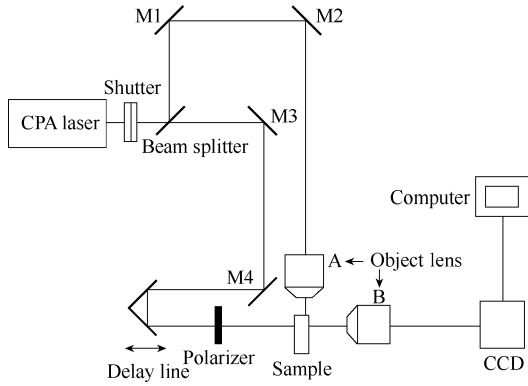


Fig. 1 The experimental setup for shadowgraph

When a weak laser passes through electron plasma, it is absorbed by inverse bremsstrahlung absorption. It can be expressed by [16]

$$\frac{dI_p}{dx} = -\sigma n_e I_p \quad (1)$$

where σ is the absorption cross section for inverse bremsstrahlung and depends on the electron collision time τ in the conduction band according to the Drude model [14]:

$$\sigma = \frac{ke^2\tau}{m_e\epsilon_0\omega[1 + (\omega\tau)^2]}$$

From Eq. (1), we can get

$$\ln(I_{p0}/I_{pd}) = \int \sigma n_e dx \quad (2)$$

Here, I_{p0} and I_{pd} represent the probe laser intensity before and after passing through the plasma region. Without the

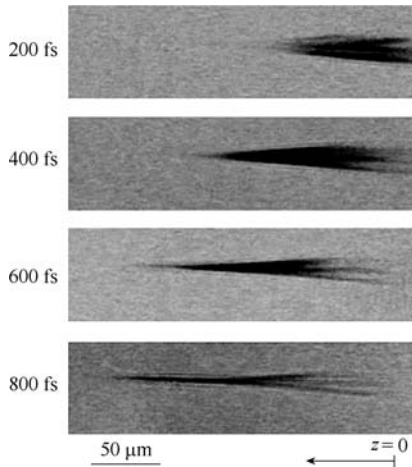


Fig. 2 Time-resolved shadowgraphs in fused silica. The input intensity is around 7×10^{13} W/cm² in focal region



Fig. 3 Interferometric image in fused silica at 400 fs delay time. The input intensity is around 7×10^{13} W/cm² in focal region

value of collision time, we cannot get the value of electron density, but we determine the relaxation of n_e from the dependence of $\ln(I_{p0}/I_{pd})$ on time delay.

When the weak laser passes through plasma, its phase is shifted by the plasma because the plasma induces a dielectric index change. The phase shift is [26]

$$\Delta\varphi = \int (n - n_0)\omega/c dx = \frac{\omega}{2cn_c} \int n_e dx \quad (3)$$

From the phase shift value, the mean electron density can be estimated. Combine Eq. (3) with Eq. (2), the electron collision time can be calculated from

$$\frac{\ln(I_{p0}/I_{pd})}{4\pi n_0 D} \frac{1 + (\omega\tau)^2}{\omega\tau} - 1 = 0 \quad (4)$$

Here, D is the ratio of fringe shift number to the interference period. When $D = 1$, the phase shift is 2π .

We used the pump-probe technique to measure the time-resolved plasma absorption and phase shift and calculated the electron density, electron collision time, and electron relaxation time.

In our experiment, the pulse duration is 130 fs, and wavelength is 800 nm. The schematic diagram of the experimental setup for time-resolved shadowgraph is shown in Fig. 1. The sample was translated to a new position after every shot. A single pulse was chosen by a shutter. The laser beam was split into pump and probe pulses by a beam splitter. An objective A (Olympus, $\times 4$,

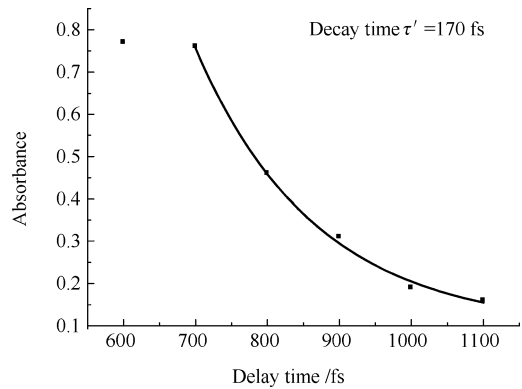


Fig. 4 Evolution of absorption of the probe due to electron plasma in fused silica. The vertical axis represents absorbance, denoted by $\ln(I_{p0}/I_{pd})$. The solid line indicates the exponential decay fitting with the decay time of 170 fs

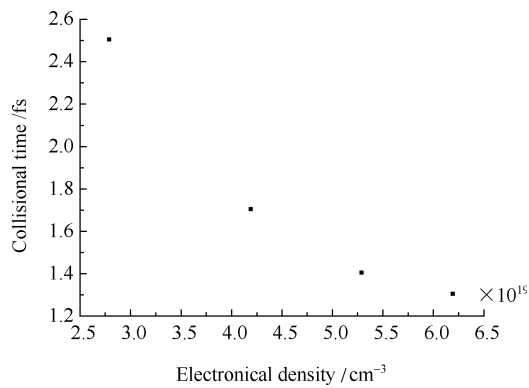


Fig. 5 Electron collision time vs mean electron density in fused silica

NA = 0.16) was used to focus the pump laser beam. After passing an optical delay stage and a polarizer, the probe beam illuminated the interaction region perpendicularly to the pump beam and was imaged onto a charge-coupled device (CCD) by another objective B ($\times 20$, NA = 0.4). A Wollaston prism and an analyzer were added after the objective B to achieve the interference fringes images. In the experiments, time zero was set when the peaks of the pump beam and the probe beam overlapped at $z = 0$.

At first, we took shadowgraphs and interference images in fused silica [19]. Figure 2 shows shadowgraphs measured at several delay times with a laser intensity of around 7×10^{13} W/cm² in the focal region [19], while Fig. 3 shows the interference image at the 400 fs time delay [19]. The pump beam was propagated from the right to the left. Considering the cylindrical symmetry of plasma density, the probe beam would undergo absorption, reflection, re-

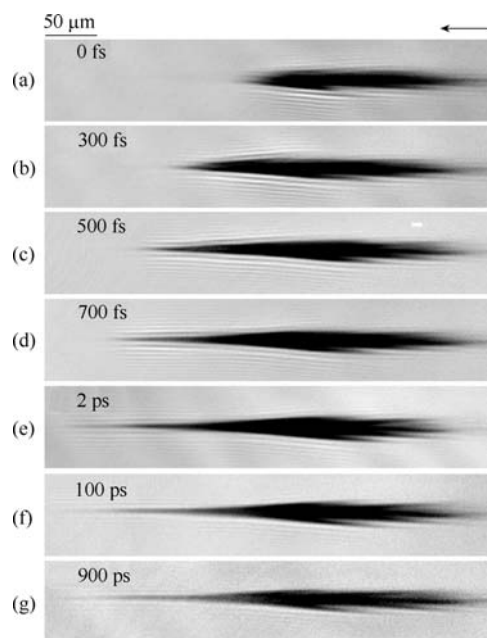


Fig. 6 Time-resolved shadowgraphs in Soda Lime glass

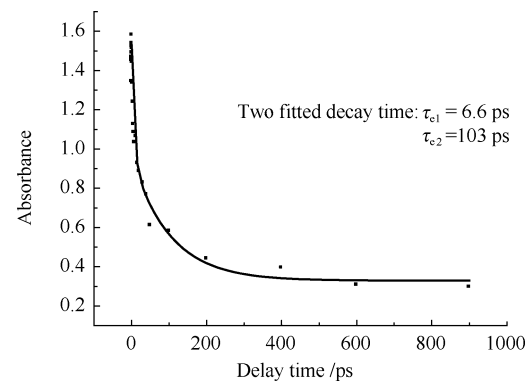


Fig. 7 Evolution of absorption of the probe due to electron plasma in Soda Lime glass at $z = 230$ μm . The vertical axis represents absorbance, denoted by $\ln(I_{p0}/I_{pd})$. The solid line indicates two-exponential decay fitting with the decay time of 6.6 and 103 ps

fraction, and phase shift. The reflection and refraction were ignored when we calculated the parameters using Eqs. (2), (3) and (4).

From the time-resolved shadowgraph, the absorbance of $\ln(I_{p0}/I_{pd})$ at $z = 119$ μm was calculated and shown in Fig. 4 [19]. From Eq. (2), it is known that this time-dependent absorbance represents the relaxation of electron density, when the change of σ or τ on electron energy is ignored.

The relaxation time can be estimated by this approximation. We found that the data points in Fig. 4 were fitted with exponential decay, and the decay time was 170 fs. Several beginning degressive data points were ignored because at that time, the electron plasma was still induced, although the total density was decreasing. We also ignored the data points for the delay time > 1.2 ps, when the thermal effect began to work. The calculated decay time at $z = 92$ μm is 125 fs, and that at other z points is between 120 and 200 fs. The difference is due to the difference of σ or collision time τ when the electron has different energy. In our experiment, the average decay time is 170 fs. This fast decay is induced by a self-trapping process [17,23,24]. The self-trapping state should locate deep below the bottom of the conduction band. The trapped electrons do not contribute to the absorption of the probe beam.

From Fig. 3, we measured the fringe shift number and the interference period and calculated the electron density. From the image, the size of the plasma can be measured. Then, the mean electron density can be calculated: 5.3×10^{19} cm⁻³ at $z = 92$ μm at the 400 fs time delay. The collision time was calculated to be 1.4 fs at the same position using the experiment data in Figs. 3 and 4. With the increase in delay time, the electron density decreased and the collision time increased. Figure 5 shows the collision time vs electron density. The electron collision time increases with the decrease in the electron density.

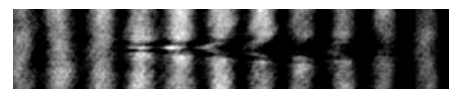


Fig. 8 Interferometric image in Soda Lime glass at 500 fs delay time

This is coincident with the result that the collision time increases with the decrease in electron energy when it is low [27].

After obtaining the plasma density, electron collision time, and plasma size, we calculated the reflection and refraction of the probe beam. It was verified that the influence of reflection and refraction of the light that passed through the middle of the plasma can be ignored.

We found that the electron relaxation time, electron density, and electron collision time in quartz are close to those in fused silica under the same input energy of the femtosecond laser pulse.

In Soda Lime glass, the electron density decay process was different from that in fused silica and quartz [25]. Figure 6 shows the time-resolved shadowgraphs, and Fig. 7 shows the absorbance decay process in Soda Lime glass [25]. It is obvious that the decay process was much slower in Soda Lime glass than that in fused silica. The decay process could be fitted as two exponential decays: $A\exp(-t/\tau_{e1}) + B\exp(-t/\tau_{e2}) + c$; and the two fitted decay times were $\tau_{e1} = 6.6$ ps and $\tau_{e2} = 103$ ps. Here, the fast decay time was regarded as electron relaxation time in the conduction band, and the slow decay time represented the lifetime of the electron in the conduction band, i.e., the recombination time of the electrons with holes. There was no fast self-trapping process as that in fused silica and quartz.

In K9 glass, the electron decay process was similar to that in Soda Lime glass. The two decay times were fitted as 4.3 and 113 ps.

Although the electron decay time in Soda Lime and K9 glass was completely different from that in quartz and fused silica, the electron collision times in these materials were similar. From the interference images shown in Fig. 8 and the shadowgraph images in Fig. 6, it was calculated that the collision time was 1.83 fs at an electron density of $6.0 \times 10^{19} \text{ cm}^{-3}$ in Soda Lime glass. In K9 glass, it was 2.8 fs at an electron density of $7.0 \times 10^{19} \text{ cm}^{-3}$ [25].

Fused silica and quartz are pure, while Soda Lime glass and K9 glass are doped. We think that it is possible that the doped ions change the electron band structure and induced the disappearance of the self-trapping state. However, the influence of the doped ions on phonon state is not so distinct, and the electron-phonon collision time has not been changed much.

In conclusion, we measured electron density, electron collision time, and electron relaxation time in fused silica, quartz, Soda Lime glass, and K9 glass. In these materials, the electron density induced by femtosecond laser pulse can reach 10^{19} cm^{-3} , and the electron collision time is about several femtoseconds. The lifetime of electrons is about 170 fs in the conduction band of quartz and fused silica because of self-trapping. The lifetime of electrons in the conduction band of Soda Lime glass and K9 glasses is about 100 ps. It is proposed that the doped ions modulate the energy band and make self-trap state disappear.

Acknowledgements This work was supported by the National Key Basic Research Special Foundation (NKBRFSF) under grant no. TG1999075207 and by the National Natural Science Foundation of China under grant nos. 10104003 and 90101027.

References

1. Glezer E.-N., Milosavljevic M., Huang L., Finlay R.-J., Her T.-H., Callan J.-P. and Mazur E., Three-dimensional optical storage inside transparent materials, *Opt. Lett.*, 1996, 21(24): 2023
2. Tzortzakakis S., L.-S., Franco M., Prade B. and Mysyrowicz A., Self-guided propagation of ultrashort IR laser pulses in fused silica, *Phys. Rev. Lett.*, 2001, 87(21): 213902
3. Davis K.-M., Miura K., Sugimoto N. and Hirao K., Writing waveguides in glass with a femtosecond laser, *Opt. Lett.*, 1996, 21(21): 1739
4. Will M., Nolte S. and Chichkov B.-N., Optical properties of waveguides fabricated in fused silica by femtosecond laser pulses, *Appl. Opt.*, 2002, 41: 4360
5. Salimina A., Nguyen N.-T. and Nadeau M.-C., Writing optical waveguides in fused silica using 1 KHz femtosecond infrared pulses, *J. Appl. Phys.*, 2003, 93: 3724
6. Watanabe W., Note Y. and Itoh K., Fabrication of multimode interference waveguides in glass by use of a femtosecond laser, *Opt. Lett.*, 2005, 30(21): 2888
7. Pertsch T., Peschel U., Lederer F., Burghoff J., Will M., Nolte S. and Tunnermann A., Discrete diffraction in two-dimensional arrays of coupled waveguides in silica, *Opt. Lett.*, 2004, 29(5): 468
8. Watanabe W., Asano T., Yamada K., Itoh K. and Nishii J., Wavelength division with three-dimensional couplers fabricated by filamentation of femtosecond laser pulses, *Opt. Lett.*, 2003, 28(24): 2491
9. Yamada K., Watanabe W., Li Y.-D., Itoh K. and Nishii J., Multilevel phase-type diffractive lenses in silica glass induced by filamentation of femtosecond laser pulses, *Opt. Lett.*, 2004, 29(16): 1846
10. Wang X., Guo H., Yang H., Jiang H. and Gong Q., Fabrication of beam shapers in the bulk of fused silica by femtosecond laser pulses, *Appl. Opt.*, 2004, 43(23): 4571
11. Li Y., Watanabe W., Itoh K. and Sun X.-D., Holographic data storage on nonphotosensitive glass with a single femtosecond laser pulse, *Appl. Phys. Lett.*, 2002, 81: 1952
12. Li Y., Itoh K., Watanabe W., Yamada K., Kuroda D., Nishii J. and Jiang Y.-Y., Three-dimensional hole drilling of silica glass from the rear surface with femtosecond laser pulses, *Opt. Lett.*, 2001, 26(23): 1912
13. Cheng Y., Sugioka K. and Kidorkawa K., Microfluidic laser embedded in glass by three-dimensional femtosecond laser microprocessing, *Opt. Lett.*, 2004, 29(17): 2007
14. Stuart B.-C., Feit M.-D., Herman S., Rubenchik A.-M., Shore B. W. and Perry M. D., Nanosecond-to-femtosecond laser-induced breakdown in dielectrics, *Phys. Rev. B*, 1996, 53(4): 1749
15. Liu Y., Jiang H., Sun Q., Wu Z., Yang H. and Gong Q., Different tendencies of breakdown threshold on pulse duration in subpicosecond regime in fused silica, *J. Opt., A Pure Appl. Opt.*, 2005, 7: 1
16. Mao X., Mao S.-S. and Russo R.-E., Imaging femtosecond laser-induced electronic excitation in glass, *Appl. Phys. Lett.*, 2003, 82: 697
17. Audebert P., Daguzan P., Santos A.-D., Gauthier J.-C., Geindre J.-P., Guizard S., Hamoniaux G., Krastev K., Martin P., Petite G. and Antonetti A., Space-time observation of an electron gas in SiO_2 , *Phys. Rev. Lett.*, 1994, 73: 1990
18. Li M., Menon S., Nibarger J.-P. and Gibson G.-N., Ultrafast electron dynamics in femtosecond optical breakdown of dielectrics, *Phys. Rev. Lett.*, 1999, 82: 2394

19. Sun Q., Jiang H.-B., Liu Y., Wu Z.-X., Yang H. and Gong Q.-H., Measurement on the collision time of dense electron plasma induced by femtosecond laser in fused silica, *Opt. Lett.*, 2005, 30: 320
20. Sudrie L., Couairon A., Franco M., Lamouroux B., Prade B., Tzortzakis S. and Mysyrowicz A., Femtosecond laser-induced damage and filamentary propagation in fused silica, *Phys. Rev. Lett.*, 2002, 89: 186601
21. Tzortzakis S., Sudrie L., Franco M., Prade B. and Mysyrowicz A., Self-guided propagation of ultrashort IR laser pulses in fused silica, *Phys. Rev. Lett.*, 2001, 87: 13902
22. Du D., Liu X., Korn G., Squier J. and Mourou G., Laser-induced breakdown by impact ionization in SiO₂ with pulse widths from 7 ns to 150 fs, *Appl. Phys. Lett.*, 1994, 64(23): 3071
23. Petite G., Daguzan P., Guizard S. and Martin P., Ultrafast processes in laser irradiated wide bandgap insulators, *Appl. Surf. Sci.*, 1997, 110: 36
24. Petite G., Guizard S., Martin P. and Quéré F., Comment on 'Ultrafast electron dynamics in femtosecond optical breakdown of dielectrics', *Phys. Rev. Lett.*, 1999, 83: 5182
25. Sun Q., Jiang H.-B., Liu Y., Zhou Y.-H., Yang H. and Gong Q.-H., Relaxation of dense electron plasma induced by femtosecond laser in dielectric materials, *Chin. Phys. Lett.* (submitted for publication)
26. Yang H., Zhang J., Li Y.-J., Zhang J., Li Y.-T., Chen Z.-L., Teng H., Wei Z.-Y. and Sheng Z.-M., Characteristics of self-guided laser plasma channels generated by femtosecond laser pulses in air, *Phys. Rev., E*, 2002, 66: 016406
27. Arnold D., Cartier E. and Dimaria D.-J., Acoustic-phonon runaway and impact ionization by hot-electrons in silica dioxide, *Phys. Rev., B*, 1992, 45(3): 1477